

Supporting Information

Redox Modulation of PTEN Phosphatase Activity by Hydrogen Peroxide and Bisperoxidovanadium Complexes

*Chang-Uk Lee, Gernot Hahne, Jonas Hanske, Tanja Bange, David Bier, Christoph Rademacher, Sven Hennig, and Tom N. Grossmann**

anie_201506338_sm_miscellaneous_information.pdf

Contents

1 SI METHODS	S2
1.1 Protein expression and purification	S2
1.2 IC ₅₀ Determination of phosphatase inhibition.....	S2
1.3 Reversibility of phosphatase inhibition	S2
1.4 Impact of tartrate on PTEN oxidation and reactivation	S3
1.5 Kinetics of phosphatase inhibition by H ₂ O ₂	S3
1.6 Phosphatase activity in presence of orthovanadate	S3
1.7 HPLC-MS	S4
1.8 X-ray crystallography and soaking.....	S4
1.9 NMR measurements.....	S5
2 TABLES AND FIGURES	S6
2.1 Protein expression and purification	S6
2.2 Phosphatase activity.....	S7
2.3 HPLC-MS	S10
Full-length PTEN	S10
Truncated PTEN.....	S12
2.4 Crystal structures.....	S14
Crystal structure PTEN (reduced).....	S14
Crystal structure PTEN + H ₂ O ₂	S18
Crystal structure PTEN + bpV-phen.....	S21
2.5 ⁵¹ V-NMR measurements.....	S25
3 REFERENCES	S27

1 SI METHODS

1.1 Protein expression and purification

All proteins used in this study have been expressed in insect cells using the Baculovirus Expression System.^[1] Full-length human *pten* (Uniprot: P60484)^[2] and truncated *pten* (tPTEN, 7-353 aa with a deletion from 286 to 309) were cloned into pFH1 vector containing *tobacco etch virus* (TEV) protease cleavage site and an *N*-terminal histidine (His₆) affinity tag leaving a protein construct with an *N*-terminal glycine. Bacmids were generated by transforming DH10bac with the corresponding plasmids, followed by the transfection of *Sf9* cells for virus generation (P1). This cell line was also used for virus amplification (P2). The proteins were overexpressed in *High Five* cells at 27 °C for 72 h following the infection with P2-virus. Cells were lysed by sonication in a buffer containing 50 mM Tris-HCl (pH 8.0), 500 mM NaCl, 5% glycerol, 5 mM beta-mercaptoethanol, and 1 mM PMSF. Cell debris was removed by centrifugation at 64,000 rcf for 1 h. The supernatant was collected and incubated with Ni-NTA Superflow resin (Qiagen®) overnight at 4 °C. The Ni-charged resins were washed twice with a buffer containing 50 mM Tris-HCl (pH 8.0), 500 mM NaCl, 5% glycerol, 20 mM imidazole, 5 mM beta-mercaptoethanol. The protein of interest was eluted with 50 mM Tris-HCl (pH 8.0), 500 mM NaCl, 5% Glycerol, 300 mM imidazole, 5 mM beta-mercaptoethanol, followed by His₆-tag cleavage with TEV-protease overnight at 4 °C. The proteins used for the biochemical assays were purified using size exclusion chromatography (HiLoad™ 16/60 Superdex™ S200 pg, GE Healthcare™) with a buffer containing 25 mM Tris-HCl (pH 8.0), 200 mM NaCl, 2 mM TCEP to be concentrated up to 20 mg/ml and then flash-frozen in liquid N₂. The proteins were stored at –80 °C. After His₆-tag cleavage, the protein used for the crystallization PTEN (7-353) Δ286-309 was subjected to buffer exchange (25 mM Tris-HCl (pH 7.0), 100 mM NaCl, 2 mM DTT). The following cationic exchange chromatography was performed against a buffer including 25 mM Tris-HCl (pH 7.0), 500 mM NaCl, 2 mM DTT (gradient to 100% in 15 column volumex). Finally, the protein was purified via size exclusion chromatography (HiLoad™ 16/60 Superdex™ S200 pg, GE Healthcare™) with a buffer containing 20 mM Tris-HCl (pH 7.5), 150 mM NaCl, 5 mM DTT. The purified protein was concentrated to 20 mg/ml, then flash-frozen in liquid N₂ and stored at –80 °C.

1.2 IC₅₀ Determination of phosphatase inhibition

IC₅₀ determinations of H₂O₂ and bpV-phen have been performed using a malachite green assay.^[3] 60 nM full-length PTEN was pre-incubated with 10-fold dilutions of H₂O₂ or bpV-phen (H₂O₂: 40 mM to 4 nM, bpV-phen: 0.3 mM to 0.3 nM - 150 nM bpV-phen was included) for 10 min, followed by addition of PI(3,4,5)P₃ diC8 (final: 50 nM PTEN, 75 μM PI(3,4,5)P₃ diC8). Enzymatic activity was monitored at 25 °C for 30 min. For measurements, aliquots of the reaction mixture were quenched with malachite green solution (Echelon Biosciences®, Salt Lake City, UT). Absorption values of malachite green were determined at 620 nm and relative PTEN activity was calculated based on released orthophosphate. IC₅₀-values with standard deviation were determined based on triplicate runs using GraphPad Prism™.

1.3 Reversibility of phosphatase inhibition

Full-length PTEN (100 μM) was pre-treated with either H₂O₂ (3.5 mM) or bpV-phen (400 μM) for 10 min. The reaction mixture was then diluted with buffer lacking reducing agents (mock) or containing DTT or

GSH (final: 5 μ M PTEN, 4 mM reducing agent) for 10 min. For activity measurements, PI(3,4,5)P₃ diC8 was added to the reaction mixture (final: 1 μ M PTEN, 75 μ M PI(3,4,5)P₃ diC8) and incubated for 30 min at 25 °C. The reaction was quenched with malachite green solution (Echelon Biosciences®, Salt Lake City, UT). Absorption values of malachite green were determined at 620 nm and relative PTEN activity was calculated based on released orthophosphate. PTEN activities are given relative to untreated protein samples (absence of inhibitor and reducing agent) that were processed analogously. Measurements were performed in triplicates and relative phosphatase activity including standard deviation was calculated using GraphPad Prism™.

1.4 Impact of tartrate on PTEN oxidation and reactivation

Full-length PTEN (50 μ M) was pre-treated with 5 mM H₂O₂ for 20 min in presence and absence of 1.5 M K/Na-tartrate. The reaction mixture was then diluted with buffer lacking reducing agents (mock) or containing DTT (final: 2.5 μ M PTEN, 4 mM DTT) for 10 min. For tartrate containing samples, the dilution buffer contained 1.5 M K/Na-tartrate. For activity measurements, PI(3,4,5)P₃ diC8 was added to the reaction mixture and diluted by a factor of 50 (final: 50 nM PTEN, 75 μ M PI(3,4,5)P₃ diC8) and incubated for 30 min at 25 °C. The reaction was quenched with malachite green solution (Echelon Biosciences®, Salt Lake City, UT). Absorption values of malachite green were determined at 620 nm and relative PTEN activity was calculated based on released orthophosphate. PTEN activities are given relative to untreated protein samples (absence of H₂O₂, tartrate and DTT) that were processed analogously. Measurements were performed in triplicates and relative phosphatase activity including standard deviation was calculated using GraphPad Prism™.

1.5 Kinetics of phosphatase inhibition by H₂O₂

Full-length PTEN (100 μ M) was incubated with H₂O₂ (2, 5 or 20 mM) for the given time ranges. The reaction mixture was then diluted with buffer lacking reducing agents (mock) or containing DTT (final: 5 μ M PTEN, 10 mM DTT) for 20 min. For activity measurements, PI(3,4,5)P₃ diC8 was added to the reaction mixture (final: 1 μ M PTEN, 75 μ M PI(3,4,5)P₃ diC8) and incubated for 30 min at 25 °C. The reaction was quenched with malachite green solution (Echelon Biosciences®, Salt Lake City, UT). Absorption values of malachite green were determined at 620 nm and relative PTEN activity was calculated based on released orthophosphate. PTEN activities are given relative to untreated protein samples (absence of H₂O₂ and DTT) that were processed analogously. Three measurements were performed in triplicates. Relative phosphatase activity including standard deviation was calculated using GraphPad Prism™.

1.6 Phosphatase activity in presence of orthovanadate

Full-length PTEN (60 nM) was treated either with protein buffer, bpV-phen (0.01 mM) or sodium orthovanadate (0.01, 0.1, 1 mM) for 10 min, followed by incubation with PI(3,4,5)P₃ diC8 (final: 50 nM PTEN, 75 μ M PI(3,4,5)P₃ diC8) for 30 min at 25 °C. The reaction was quenched with malachite green solution (Echelon Biosciences®, Salt Lake City, UT). Absorption values of malachite green were determined at 620 nm. PTEN activity was calculated based on released orthophosphate relative to the untreated control. Measurements were performed in triplicates and relative phosphatase activity including standard deviation was calculated using GraphPad Prism™.

1.7 HPLC-MS

100 μ M of full-length PTEN or tPTEN were treated with protein buffer including 1 mM H₂O₂ or 1 mM bpV-phen for 10 min. Both protein constructs were subsequently incubated with 2 mM iodoacetamide for 10 min, denatured in 8 M Urea and then directly digested. First, LysC (Wako™, Osaka, Japan) was used for 3 hours (protein-to-enzyme ratio 50:1) and after dilution with 4 volumes of 50 mM ammonium bicarbonate (AMBIC, pH 8.3) to a final concentration of 2.0 M urea, peptides were digested overnight at 37 °C with sequencing-grade modified trypsin (Promega™, Madison, WI; protein-to-enzyme ratio 50:1). Peptides were desalted on C18 stage tips^[4] and 100-300 ng of peptide were injected per MS run. In addition, 300 ng of peptides (untreated, bpV-phen treated and H₂O₂ treated) were treated with 10 mM DTT and 55 mM iodoacetamide to reduce existing disulfidbridges and injected afterwards. Peptides were separated on a Thermo Scientific™ EASY-nLC 1000 HPLC system (Thermo Fisher Scientific™, Odense, Denmark). Columns (75 μ m inner diameter, 20 cm length) were in-house packed with 1.9 μ m C18 particles (Dr. Maisch GmbH, Ammerbuch-Entringen, Germany). Peptides were loaded in buffer A (ddH₂O, 0.1% formic acid) and separated with a gradient from 5 to 60% buffer B (acetonitril, 0.1% formic acid) within 50 min at 200 nl/min (column temperature: 40 °C). A quadrupole Orbitrap mass spectrometer^[5] (Q Exactive™, Thermo Fisher Scientific™) was directly coupled to the liquid chromatography via a nano-electrospray source. The Q Exactive™ was operated in the data-dependent mode (survey scan range: 300-1650 m/z, with a resolution of 70,000 at m/z 200). Up to the 10 most abundant isotope patterns with a charge ≥ 2 were subjected to higher-energy collisional dissociation (normalized collision energy: 25, isolation window: 2 Th, resolution: 17,500 at m/z 200).^[6] Dynamic exclusion of sequenced peptides was switched off. Thresholds for ion injection time and ion target values were set to 20 ms and 3×10^6 for the survey scans and to 60 ms and 10^6 for the MS/MS scans. Data were acquired using Xcalibur™ software (Thermo Scientific™). To process MS raw files, MaxQuant software (version 1.5.2.18) was used.^[7] We applied the Andromeda search engine (integrated into MaxQuant) to search MS/MS spectra against the sequence of full-length PTEN. Enzyme specificity was set to trypsin allowing cleavage N-terminal to proline and up to two miscleavages. Peptides with a minimum length of seven amino acids were considered. Carbamidomethylation of cysteine and oxidation of methionine were set as variable modifications. In addition, the mass of the peptide (aa 65-72 IYNLAECR) containing cysteine C71 connected to another peptide via a disulfide bridge has been given as variable modification (elemental composition for the database search C₄₂H₆₆N₁₂O₁₃₁S). A false discovery rate (FDR) cut off of 1% was applied at the peptide, protein levels and the site decoy fraction. Initial precursor mass deviation of up to 4.5 ppm and fragment mass deviation up to 20 ppm were allowed. Precursor ion mass accuracy was improved by time-dependent recalibration algorithms in MaxQuant.

1.8 X-ray crystallography and soaking

Protein crystals of tPTEN were obtained at 20 °C by the hanging-drop vapor diffusion method from a 1:1 mixture of the protein solution (20 mg/ml) and the buffer containing 100 mM MES (pH 6.5), 1.25 M Na/K L(+)-tartrate and 7.5% glycerol. Crystals appeared after 2 days and were grown up to 5 days. Reduced PTEN crystals were flash-frozen in liquid N₂ after soaking in the cryo solution (crystallization buffer supplemented with 25% glycerol). For the crystal structure of oxidized PTEN, crystals were soaked with the crystallization buffer supplemented with 1 mM H₂O₂ for 1 h, or with 1 mM bpV-phen for 4 h. After soaking, crystals were back-soaked with cryo solution for 10 min and then flash-frozen in liquid N₂. X-ray data was collected at the Swiss Light Source (Villigen, Switzerland) at beamline PXII. The

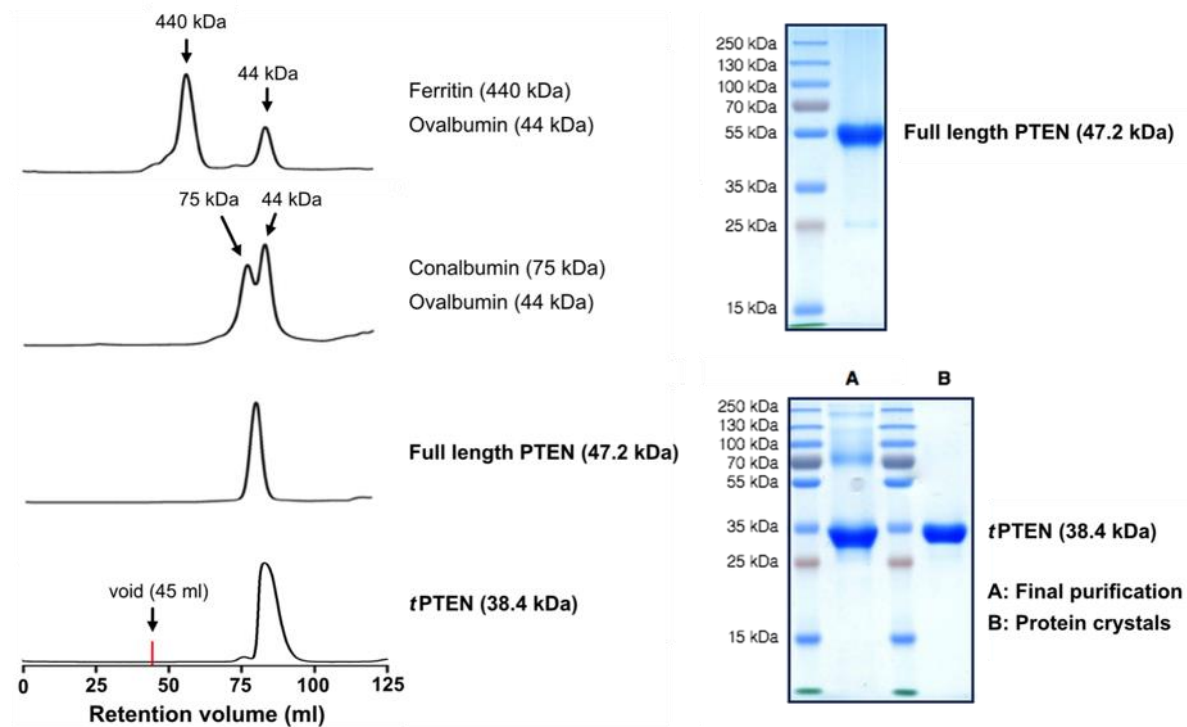
data-sets were processed using XDS^[8] providing space group C222₁ (SG No. 20) and unit cell constants ($a = 206 \text{ \AA}$, $b = 206 \text{ \AA}$, $c = 89 \text{ \AA}$; $\alpha = 90^\circ$, $\beta = 90^\circ$, $\gamma = 90^\circ$). The structures were solved by molecular replacement against the known structure of truncated PTEN (PDB^[9]: 1D5R) using PhaserMR (CCP4 suite)^[10,11]. Final structural models were built with Coot^[12] and refined using Refmac^[13] with the detwin function. Processing and refinement statistics are summarized in Table 1-3. $2 F_o - F_c$ omit map and anomalous electron density maps were generated using Sfcheck, Refmac, Cad, FFT (CCP4 suite)^[10,11]. All structural figures were represented with Pymol.^[14]

1.9 NMR measurements

NMR samples were prepared to a final volume of 150 μL and measured in 3 mm NMR tubes (Norell®, buffer: 25 mM Tris-HCl (pH 8.0) containing additional 15% D₂O, 200 mM NaCl). Reduced or pre-oxidized full-length PTEN (100 μM) was titrated with increasing concentrations of bpV-phen and sodium orthovanadate, respectively (from 50 to 200 μM). As a control, sodium orthovanadate was also measured at these concentrations in absence of protein. All ⁵¹V-NMR measurements were performed at 298 K on an Agilent® VNMR™ 600 MHz spectrometer equipped with an OneNMR 5 mm dual resonance probe, using a single 90° pulse sequence with 0.15 s acquisition time and an inter-pulse delay of 0.01 s. Scans varied from 4096 to 32716 depending on inhibitor concentration. The transmitter offset was set to -700 ppm and 500 ppm spectral width. Spectra were externally referenced to VOCl₃ (spectrometer reference) and processed in MestreNova (MestreLab) using a 9th order Bernstein polynomial baseline correction and a line-broadening of 25 Hz or 15 Hz depending on noise level.

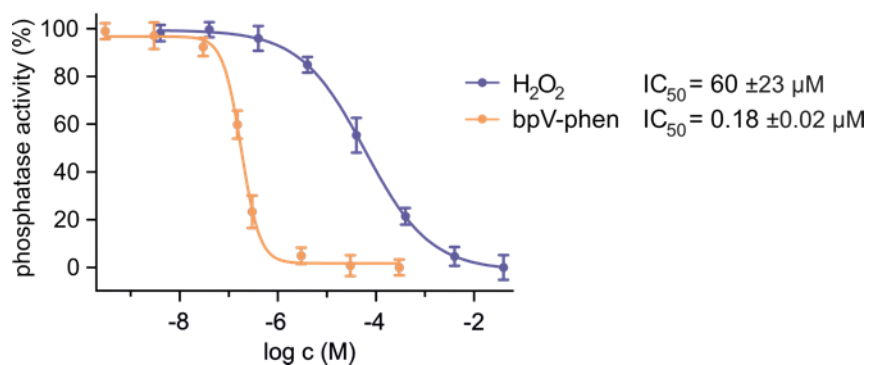
2 TABLES AND FIGURES

2.1 Protein expression and purification

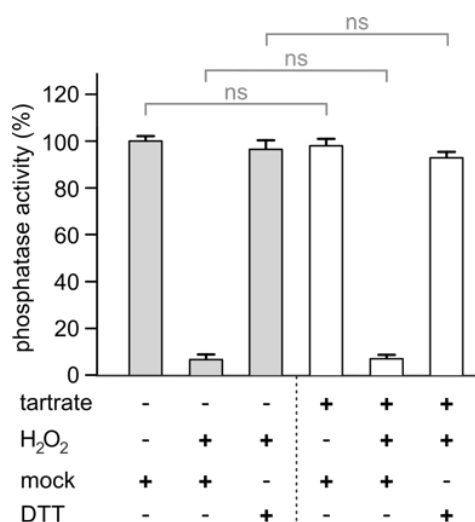


Supporting Figure S1: Chromatograms of size exclusion chromatography and SDS-PAGE of full-length PTEN and tPTEN. Full-length PTEN and tPTEN were purified via size exclusion chromatography (HiLoad 16/60 Superdex S200 pg) in the final purification step. The chromatograms of both protein constructs are represented along with that of the protein standards ferritin (440 kDa), conalbumin (75 kDa), Ovalbumin (44 kDa). SDS-PAGE of purified full-length PTEN and tPTEN (A) as well as that of protein crystals (B) verify high purity.

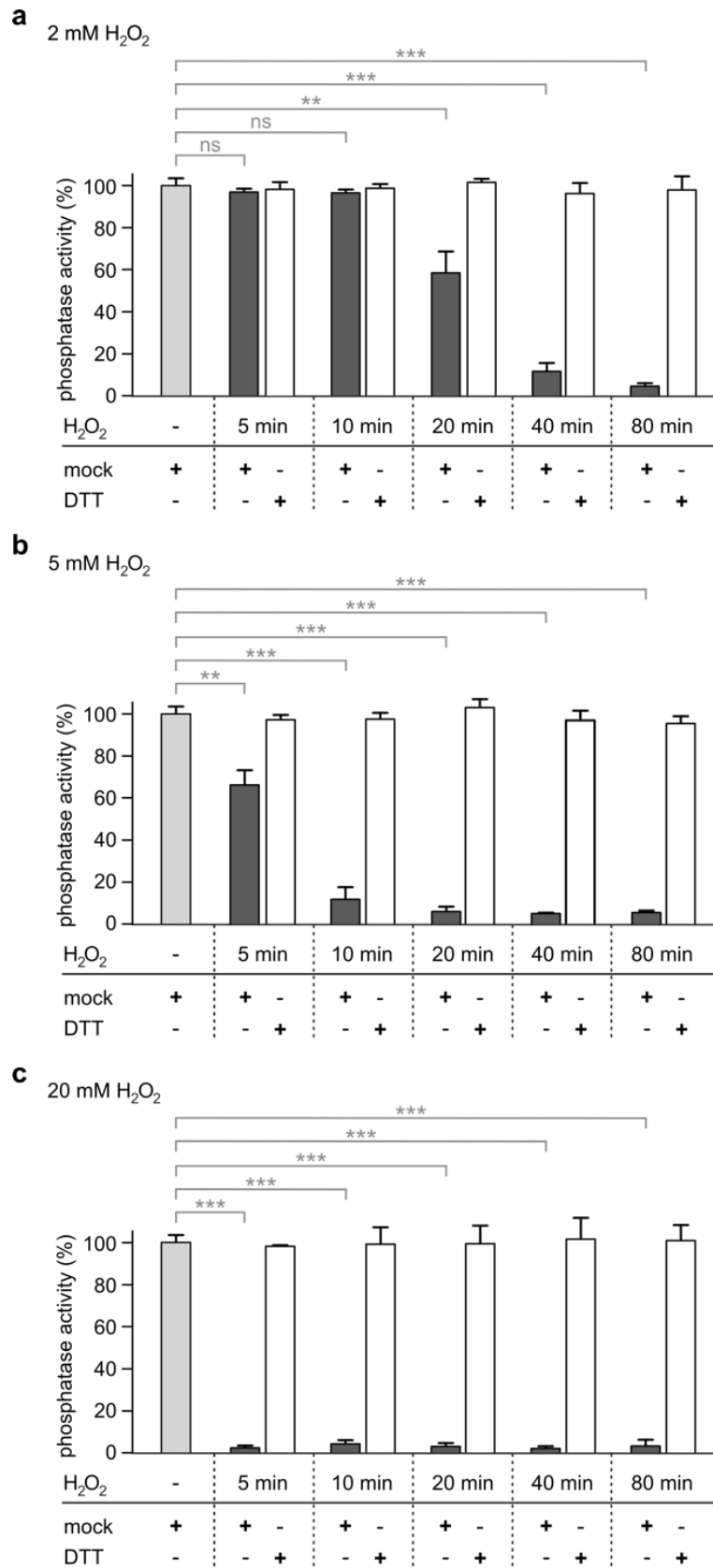
2.2 Phosphatase activity



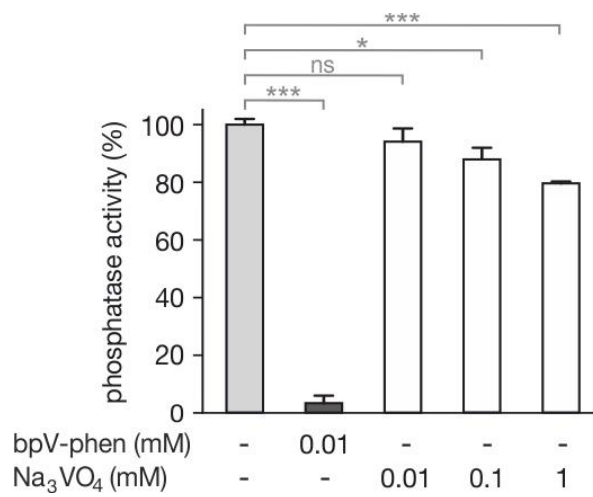
Supporting Figure S2 | IC_{50} determination. Relative phosphatase activities of PTEN with IC_{50} -values were determined using a malachite green assay with 50 nM full-length PTEN and 75 μM $\text{PI}(3,4,5)\text{P}_3$ as substrate at 25°C (triplicates, errors account for 1σ).



Supporting Figure S3 | Under our assay conditions, tartrate does not affect the oxidation and reactivation of PTEN. Effects of tartrate on oxidative inhibition and reactivation of PTEN were investigated. PTEN (50 μM) was incubated with H_2O_2 (5 mM, 20 min) in buffer (gray) or buffer containing tartrate (1.5 M, white), followed by 10 min treatment with buffer lacking reducing agents or containing 4 mM DTT. Phosphatase activities are given relative to untreated protein samples (absence of H_2O_2 , tartrate and DTT). Errors account for 1σ (triplicates; ns: $P > 0.05$).



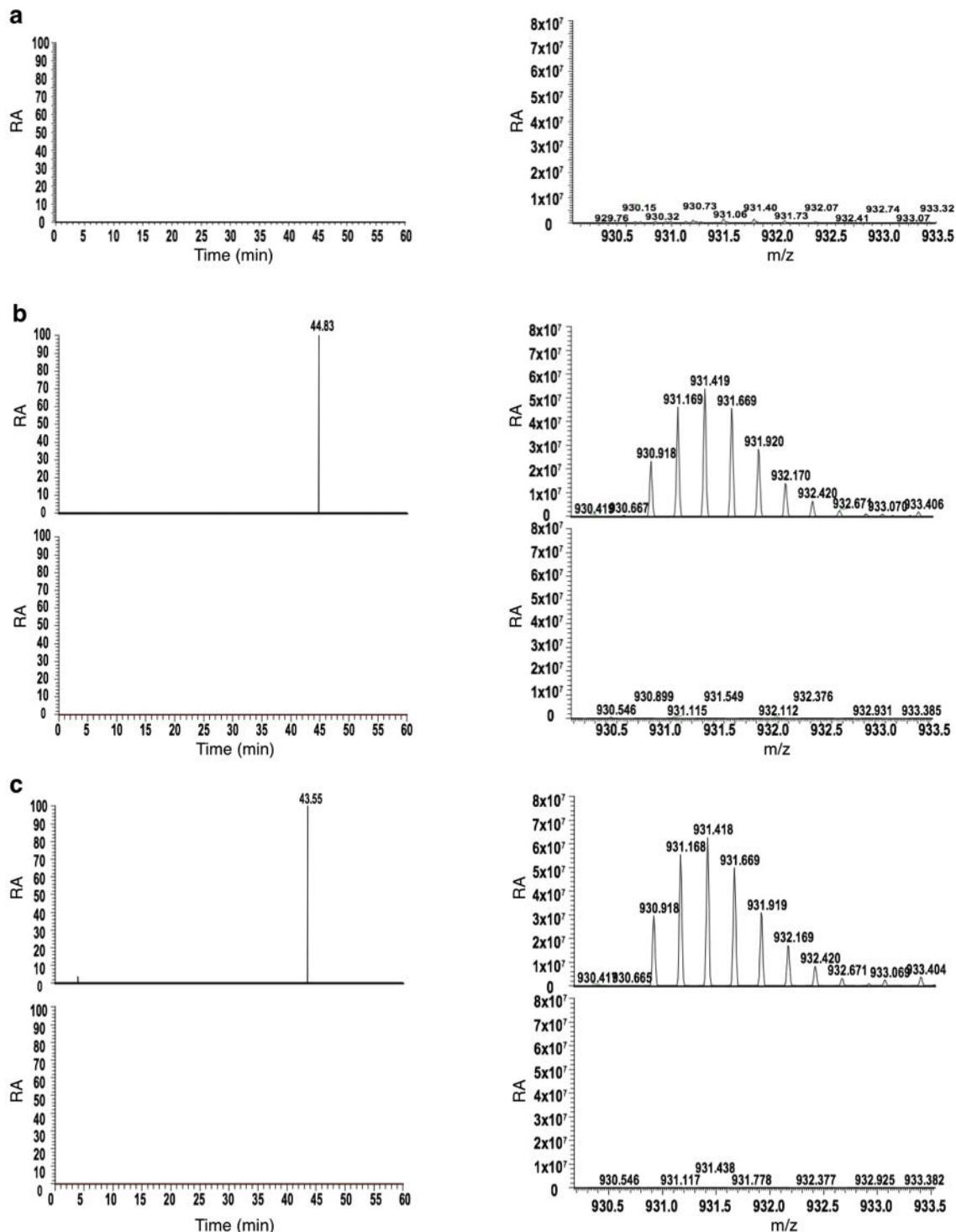
Supporting Figure S4: Reductive reactivation of PTEN after H₂O₂ treatment. a,b,c) Inhibitory effects of H₂O₂ on PTEN were investigated in a concentration- and time-dependent manner. PTEN (100 μM) was incubated with H₂O₂ (a: 2 mM, b: 5 mM, c: 20 mM), followed by 10 min treatment with buffer lacking reducing agent (dark gray) or containing 4 mM DTT (white). Errors account for 1σ (measurement: triplicate of triplicates; ns: $P > 0.05$, * $P < 0.05$, ** $P < 0.01$, *** $P < 0.001$).



Supporting Figure S5: Orthovanadate does not contribute to PTEN inhibition. Inhibitory effect of orthovanadate was tested using malachite green assay with 50 nM full-length PTEN that was treated either by bpV-phen or Na₃VO₄ (T = 25°C, t = 10 min) Errors account for 1σ (triplicates; ns: $P > 0.05$, * $P < 0.05$, ** $P < 0.01$, *** $P < 0.001$).

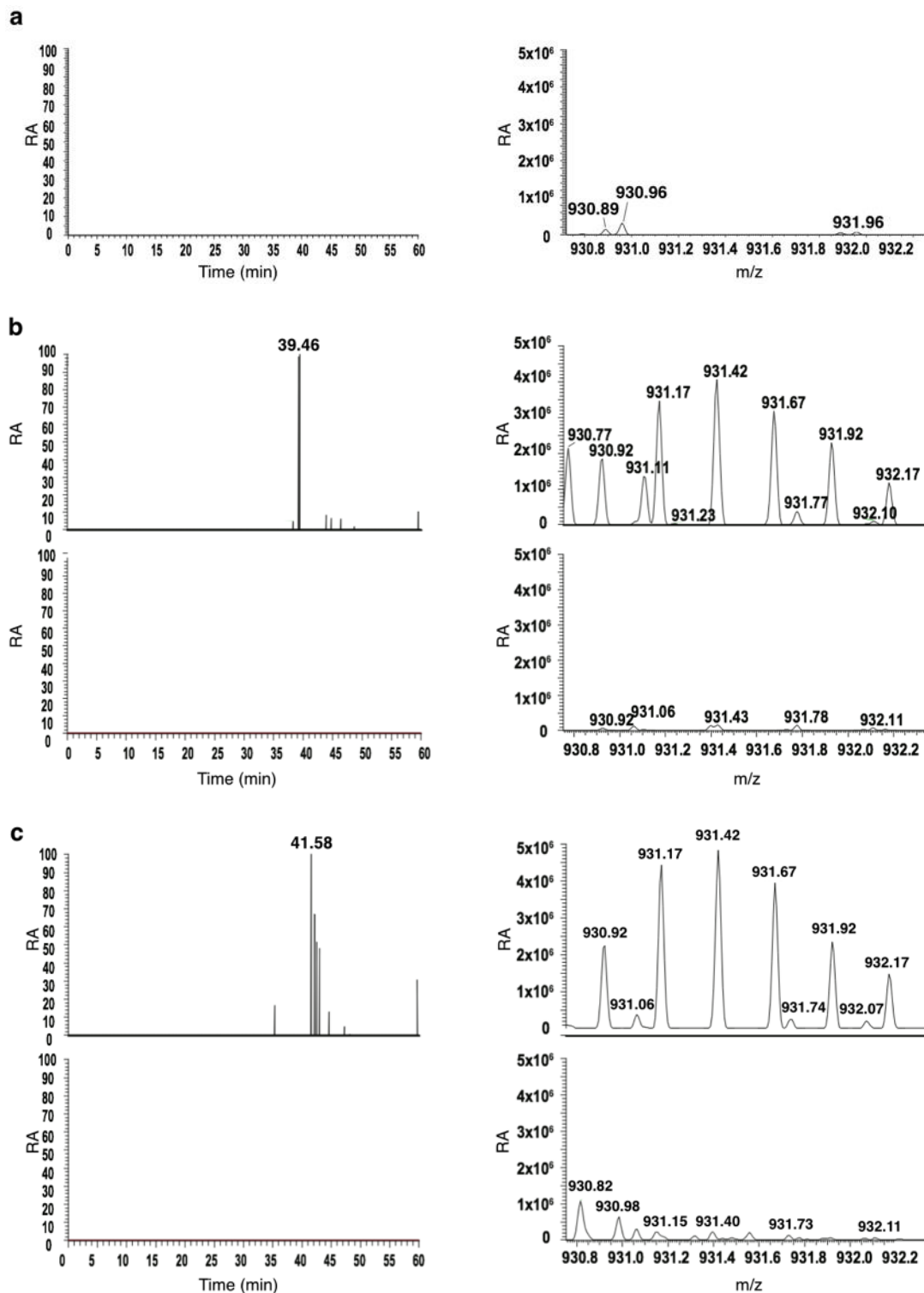
2.3 HPLC-MS

Full-length PTEN

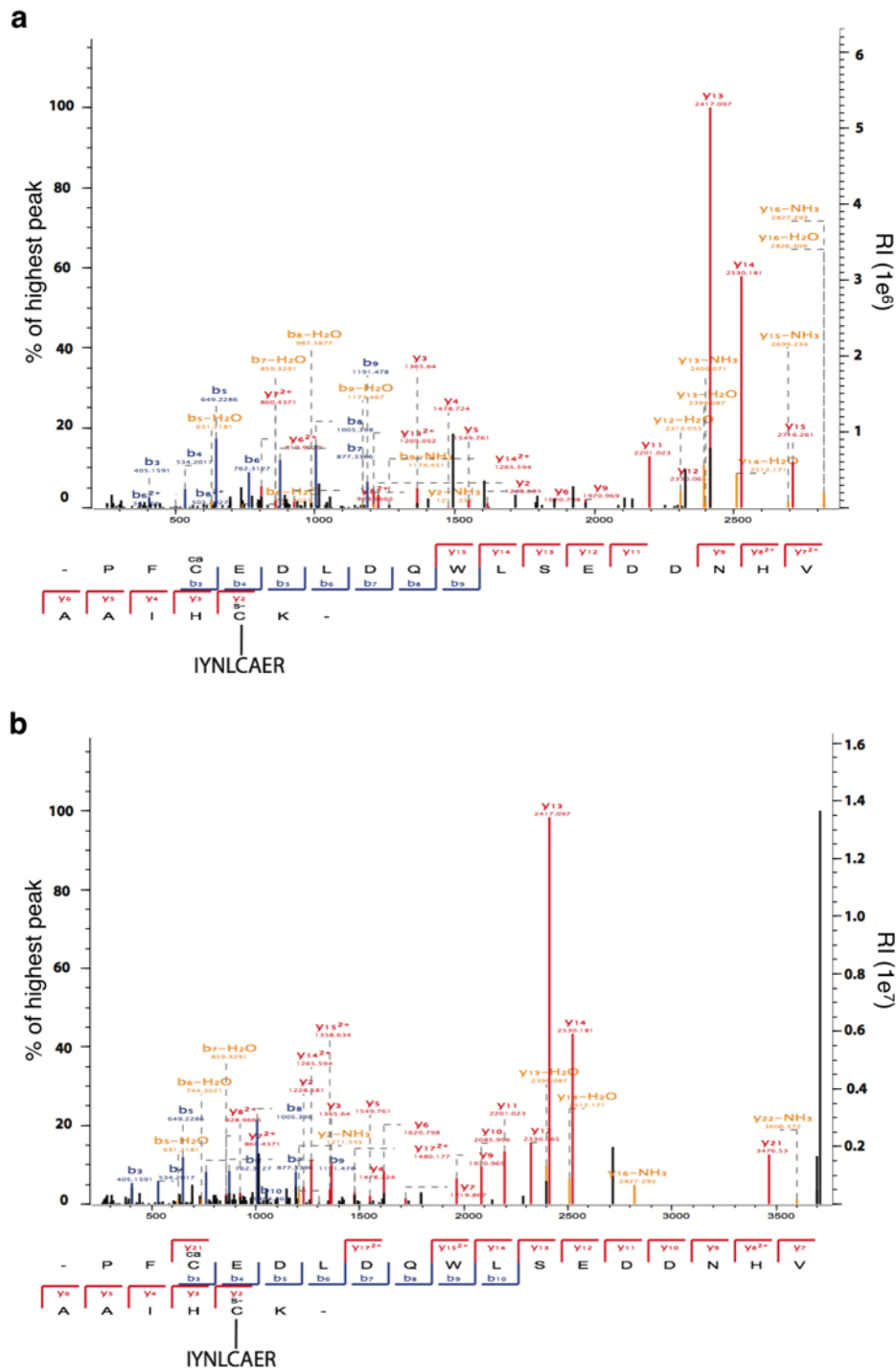


Supporting Figure S6: Detection of a disulfide between C71 and C124 in full-length PTEN by HPLC-coupled high resolution mass spectrometry. Full-length PTEN was treated with 1 mM H_2O_2 (b) or 1 mM bpV-phen (c) ($T = 25^\circ C$, $100 \mu M$ PTEN, $t = 10$ min). Disulfide formation was validated by mass spectrometric analysis. The eluting peak of the disulfide-bridged tryptic fragment in HPLC and the corresponding high resolution MS-spectra (mass error < 1 ppm) are shown in the left and right panel, respectively. The tryptic fragment is absent in the untreated control (a) and after incubation with 10 mM DTT (b and c, lower panel).

Truncated PTEN



Supporting Figure S8: Detection of a disulfide between C71 and C124 in tPTEN by HPLC-coupled high resolution mass spectrometry. tPTEN was treated with 1 mM H₂O₂ (b) or 1 mM bpV-phen (c) (T = 25°C, 100 μM PTEN, t = 10 min). Disulfide formation was validated by mass spectrometric analysis. Elution peak of the disulfide-bridged tryptic fragment in HPLC and the corresponding high resolution MS-spectra (mass error < 1 ppm) are shown in the left and right panel, respectively. The fragment is absent in the untreated control (a) and after incubation with 10 mM DTT (b and c, lower panel).



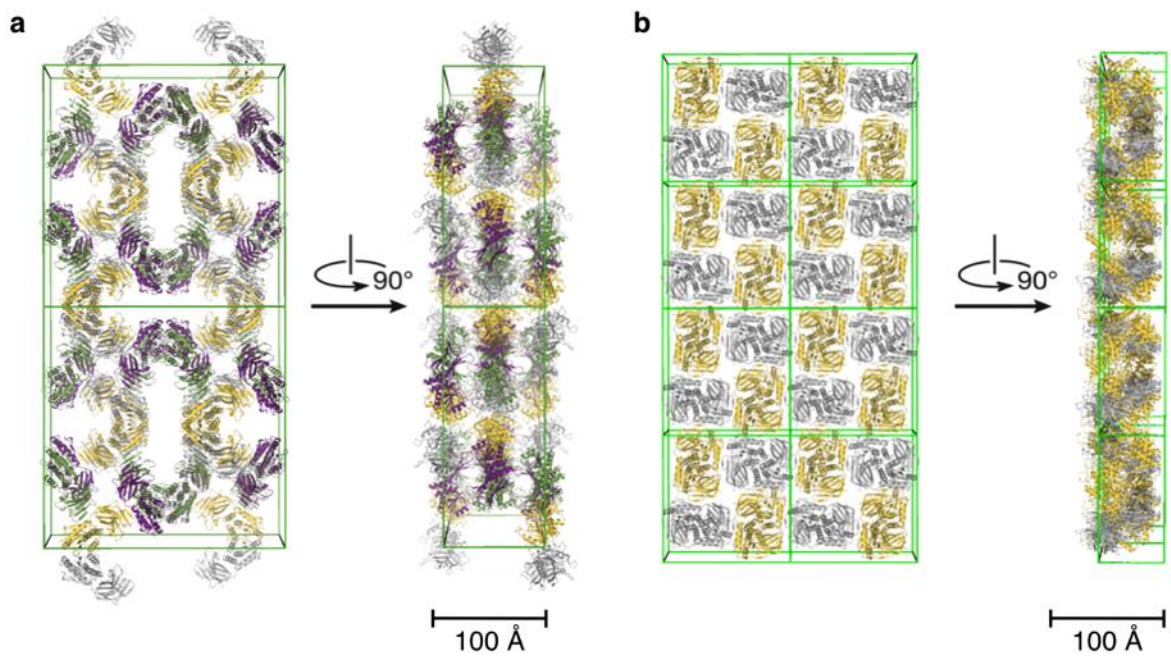
Supporting Figure S9: MS/MS spectra of disulfide-bridged peptide of *t*PTEN. Analogous to the full-length PTEN (Figure S4), *t*PTEN undergoes disulfide formation between C71 and C124 after treatment with a) H₂O₂ or b) bpV-phen. The spectra show the annotated disulfide-bridged peptides of C71-containing IYNLCAER cross-linked to a peptide fragment including C124. Overall, the tryptic fragment has been sequenced over 300 times.

2.4 Crystal structures

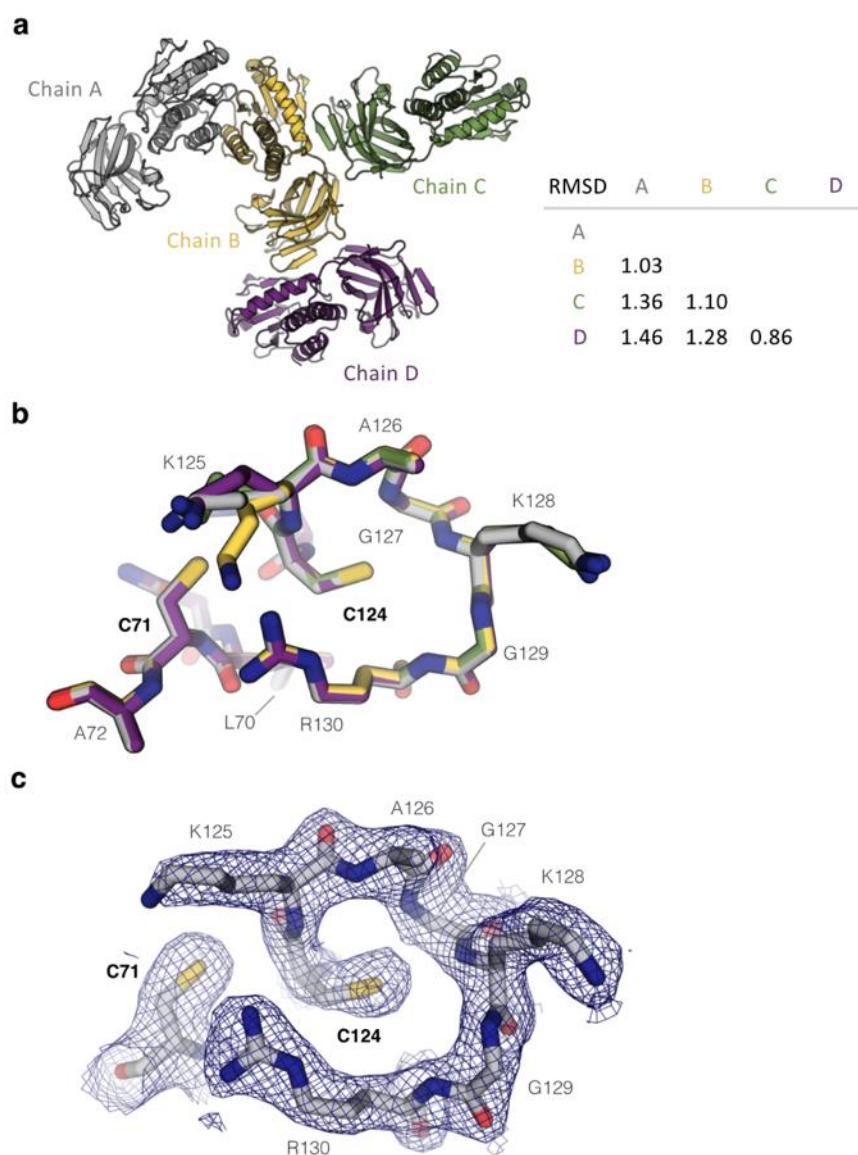
Crystal structure PTEN (reduced)

	tPTEN
PDB code	5BZZ
Data Collection	
Space group	C222 ₁
Unit-cell parameters	
a, b, c (Å)	207.17, 207.39, 87.78
α, β, γ (°)	90, 90, 90
Wavelength (Å)	1.000010
Resolution limits (Å)	46.36 - 2.20 (2.30 - 2.20)
No. of unique reflections	95899 (11832)
Completeness (%)	99.9 (99.9)
Multiplicity	13.48 (13.79)
I/ σ I	13.96 (1.17)
CC _{1/2}	99.9 (72.7)
R _{obs}	15.0 (263.7)
Refinement	
Resolution limits (Å)	46.36 - 2.20 (2.30 - 2.20)
R _{Work} / R _{Free}	0.1920 / 0.2207
R.m.s.d.	
Bond length (Å)	0.0094
Bond angles (°)	1.567
B-factors (Å ²)	61.4
No. atoms	
Protein	10338
Ligand	40
Water	890
Ramachandran plot (%)	
Favored regions	92.9
Allowed regions	6.2
Disallowed regions	0.9

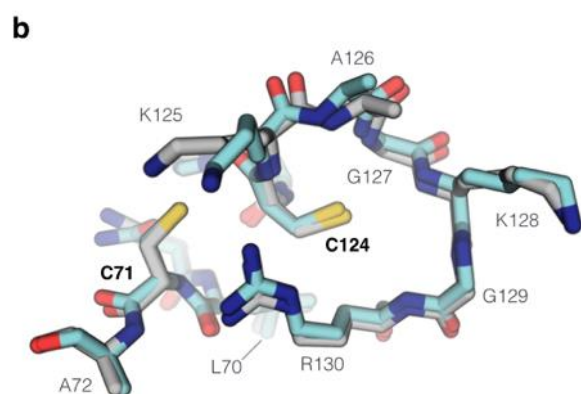
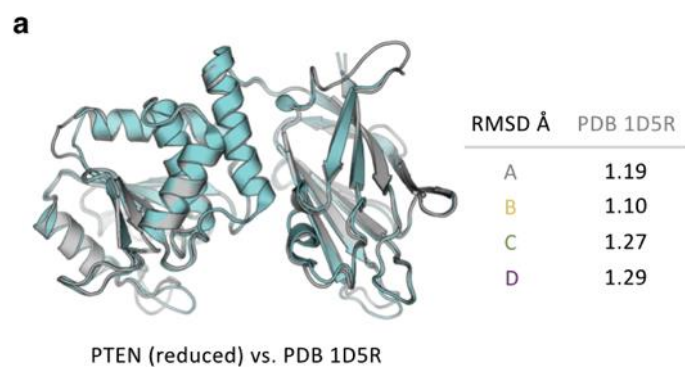
Supporting Table S1: Data collection and refinement statistics of PTEN crystal (reduced). Atomic coordinates of each structure were deposited in the RCSB Protein Data Bank with the indicated accession codes. Values in parenthesis correspond to the highest resolution shell. CC_{1/2} reflects the percentage of correlation between intensities from random half-datasets. ^[15] R_{Free} was calculated by omitting 5% of the reflections from refinement.



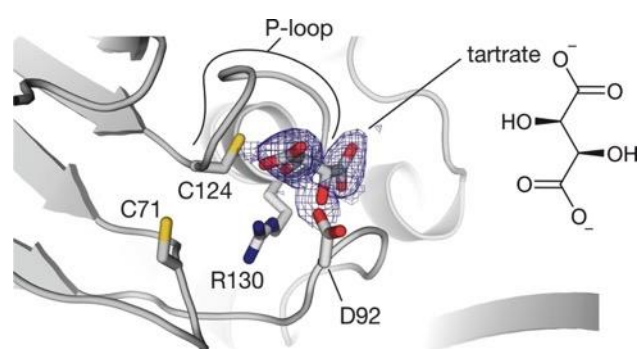
Supporting Figure S10: Novel crystal packing of PTEN in unit cells compared with the previous structure. a) Front and side views of the lattice packing of reduced *t*PTEN. Four molecules (chain A: gray, B: yellow, C: green, D: purple) are present per asymmetric unit (space group $C222_1$). b) Front and side views of the lattice packing of the previously reported PTEN crystal structure (PDB code 1D5R).^[16] Two molecules (chain A: gray, B: yellow) are assigned to an asymmetric unit (space group $I4$). A green outlined lattice displays one unit cell. The size of the unit cells is adjusted to the scale shown in the figure.



Supporting Figure S11: Four molecules per asymmetric unit. a) Four molecules are present in an asymmetric unit (chain A: gray, B: yellow, C: green, D: purple). Structures show high similarity, as reflected by RMSD (314 C_{α} atoms). b) The four molecules are superimposed with a focus on the active site P-loop which aligns very closely. c) $2F_o - F_c$ electron density for the active site. The electron density of the catalytic cysteine C124 and the closely aligned cysteine C71 is disconnected. Both thiols face towards the active site.



Supporting Figure S12: Overlay of reduced PTEN with the previously reported crystal structure PDB 1D5R. a) Superimposed overall structures of reduced PTEN (gray, chain A) and PDB 1D5R (cyan, chain A) show high similarity, as reflected by RMSD (307 C_{α} atoms). b) The active site P-loop and the cysteine partner C71 of the reduced PTEN align closely with that of PDB 1D5R. Chain A of each crystal structure is shown as a representative example.

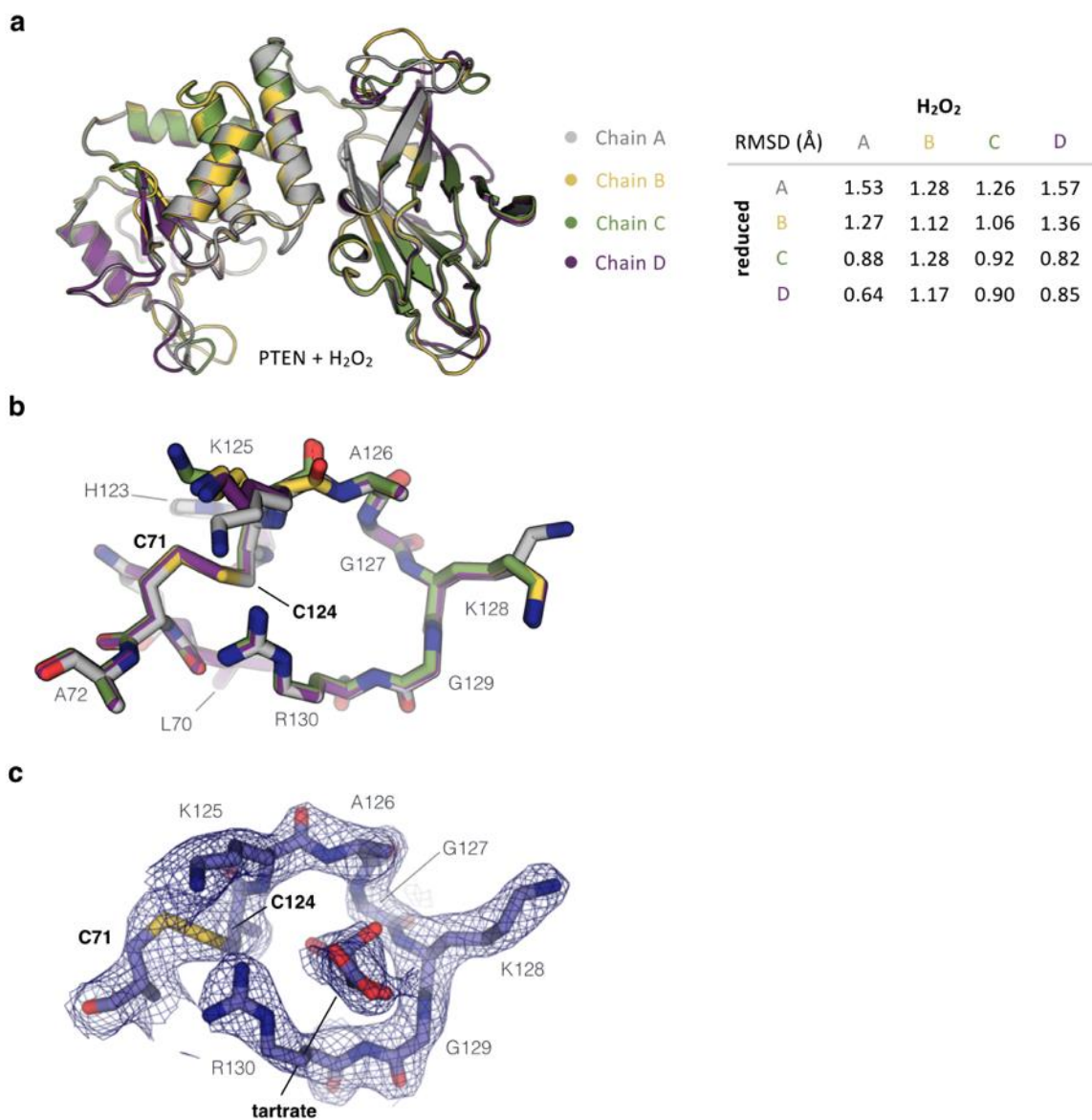


Supporting Figure S13: Crystal structure of truncated PTEN. Zoom in of active site with side chains of C71, D92, C124 and R130 shown explicitly (chain A). Active site harbors L-tartrate (mesh: $2 F_o - F_c$ electron density omit map contoured at 1σ).

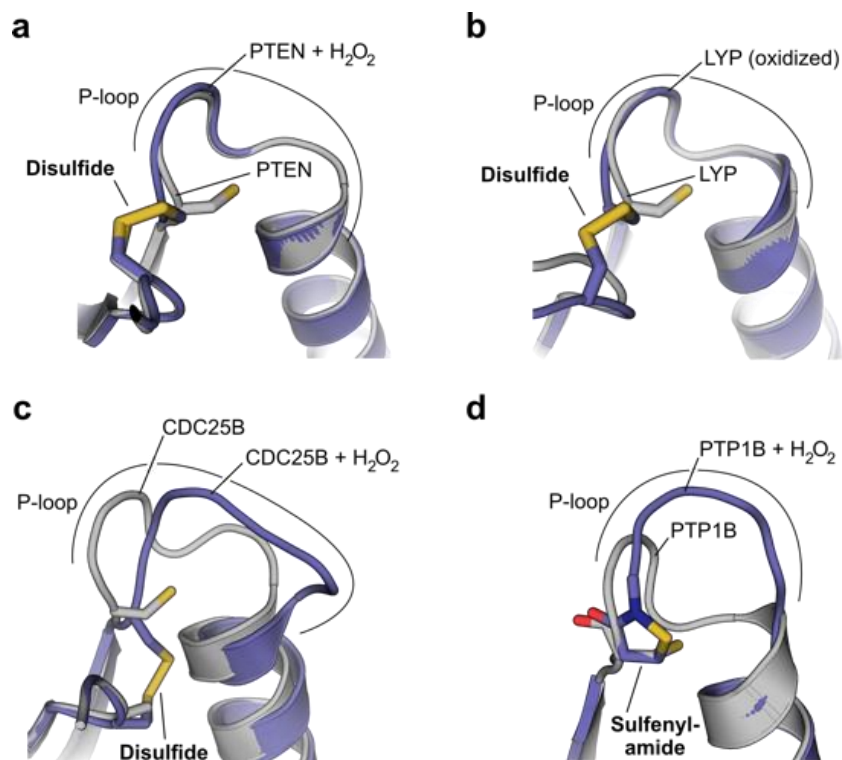
Crystal structure PTEN + H₂O₂

	tPTEN + H₂O₂
PDB code	5BUG
Data Collection	
Space group	C222 ₁
Unit-cell parameters	
a, b, c (Å)	206.87, 206.83, 87.43
α, β, γ (°)	90, 90, 90
Wavelength (Å)	1.000010
Resolution limits (Å)	48.76 - 2.40 (2.50 - 2.40)
No. of unique reflections	73497 (8347)
Completeness (%)	100 (100)
Multiplicity	11.99 (11.41)
I/σI	19.82 (1.59)
CC _{1/2}	99.9 (77.6)
R _{obs}	10.0 (158.5)
Refinement	
Resolution limits (Å)	48.76 - 2.4 (2.5 - 2.4)
R _{Work} / R _{Free}	0.1751 / 0.2106
R.m.s.d.	
Bond length (Å)	0.0100
Bond angles (°)	1.6794
B-factors (Å ²)	70.2
No. atoms	
Protein	10338
Ligand	40
Water	751
Ramachandran plot (%)	
Favored regions	93.5
Allowed regions	5.7
Disallowed regions	0.8

Supporting Table S2: Data collection and refinement statistics of H₂O₂-treated PTEN crystal (oxidized). Atomic coordinates of each structure were deposited in the RCSB Protein Data Bank with the indicated accession codes. Values in parenthesis correspond to the highest resolution shell. CC_{1/2} reflects the percentage of correlation between intensities from random half-datasets.^[15] R_{Free} was calculated by omitting 5% of the reflections from refinement.



Supporting Figure S14: Crystal structure and $2F_o - F_c$ electron density map of H₂O₂-treated PTEN. a) Four per asymmetric unit are superimposed. Overall structures show high similarity to each other. The H₂O₂-treated PTEN structures are also comparable to the reduced ones, as reflected by RMSD (314 C_α atoms). b) Superimposition of the active sites indicates very high similarity between the four molecules per asymmetric unit. c) $2F_o - F_c$ electron density map of active site (chain A) showing disulfide formation upon exposure to H₂O₂.

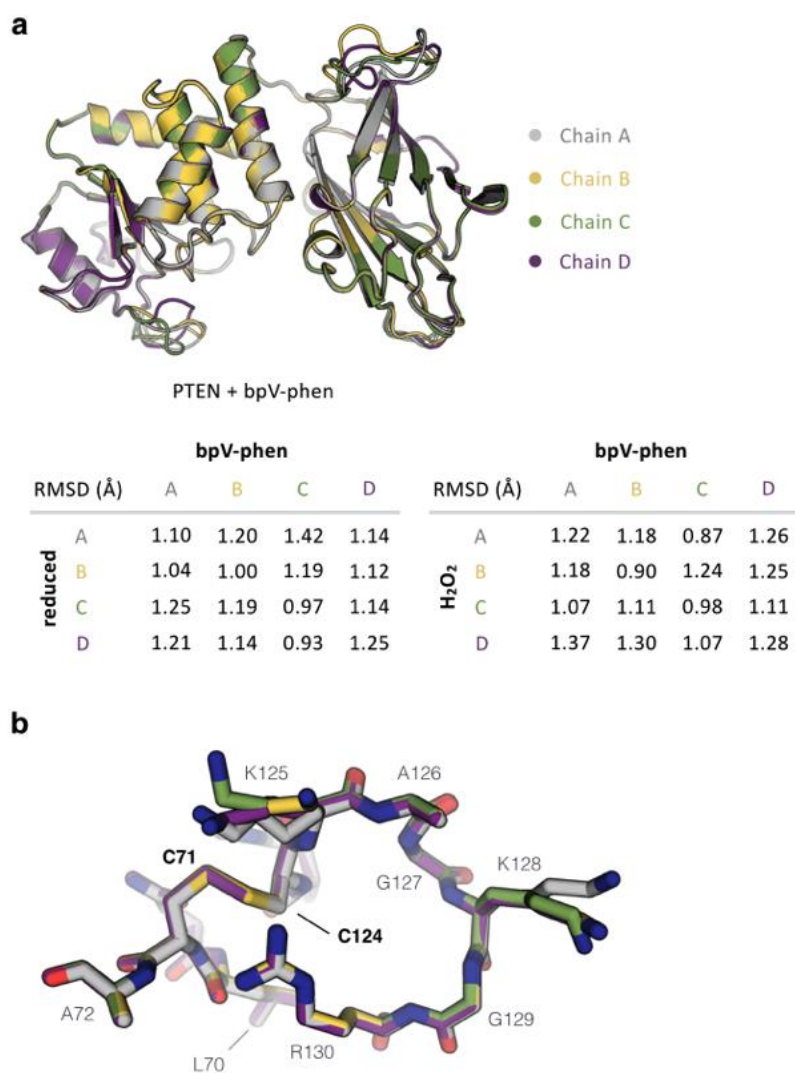


Supporting Figure S15: Structural comparison of active site P-loops upon exposure to H_2O_2 . a) H_2O_2 treatment of PTEN crystals promotes disulfide formation without major structural changes. b) Lymphoid tyrosine phosphatase undergoes disulfide formation lacking significant conformational changes in P-loop. (PDB: 2P6X, 3H2X).^[17,18] c) Oxidation with H_2O_2 distorts the active site P-loop of CDC25B via disulfide formation (PDB: 1YMK, 1YS0).^[19] d) Upon exposure to H_2O_2 , the active site P-loop undergoes a significant conformational change via sulfenyl-amide formation (PDB: 2HNP, 1OEM).^[20,21]

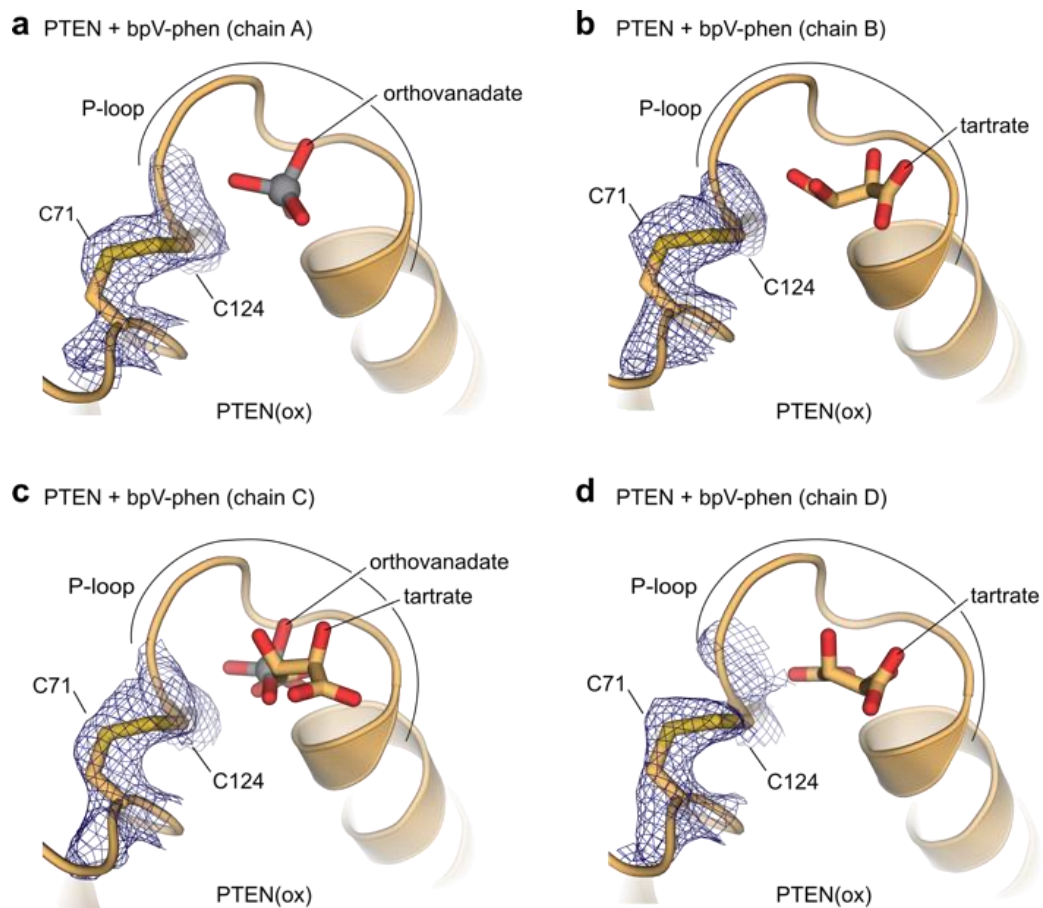
Crystal structure PTEN + bpV-phen

	tPTEN + bpV-phen
PDB code	5BZX
Data Collection	
Space group	C222 ₁
Unit-cell parameters	
a, b, c (Å)	207.06, 206.90, 87.67
α, β, γ (°)	90, 90, 90
Wavelength (Å)	1.771190
Resolution limits (Å)	46.29 - 2.50 (2.60 - 2.50)
No. of unique reflections	65393 (7145)
Completeness (%)	100 (100)
Multiplicity	12.91 (12.27)
I/ σ I	17.43 (1.53)
CC _{1/2}	99.9 (73.1)
R _{obs}	11.8 (155.2)
Refinement	
Resolution limits (Å)	46.29 - 2.50 (2.60 - 2.50)
R _{Work} / R _{Free}	0.1752 / 0.2037
R.m.s.d.	
Bond length (Å)	0.0094
Bond angles (°)	1.5376
B-factors (Å ²)	72.0
No. atoms	
Protein	10310
Ligand	40
Water	880
Ramachandran plot (%)	
Favored regions	92.8
Allowed regions	6.7
Disallowed regions	0.6

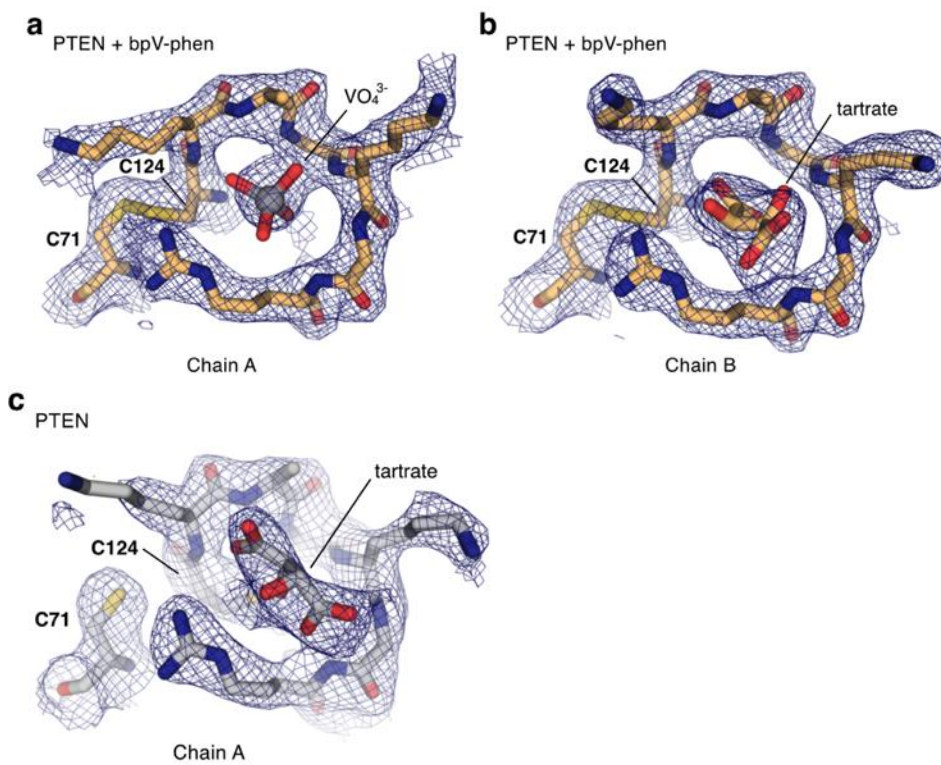
Supporting Table S3: Data collection and refinement statistics of bpV-phen-treated PTEN crystal (oxidized). Atomic coordinates of each structure were deposited in the RCSB Protein Data Bank with the indicated accession codes. Values in parenthesis correspond to the highest resolution shell. CC_{1/2} reflects the percentage of correlation between intensities from random half-datasets.^[15] R_{Free} was calculated by omitting 5% of the reflections from refinement.



Supporting Figure S16: Overlay of four bpV-phen-treated PTEN molecules per asymmetric unit. a) The four molecules per asymmetric unit are superimposed. The overall structures show high similarity to each other. The overall structure of bpV-phen-treated PTEN is very similar to the reduced and H₂O₂-treated ones, as reflected by RMSD (314 C_α atoms). b) The overlay of the active site indicates very similar conformations among the four molecules per asymmetric unit.

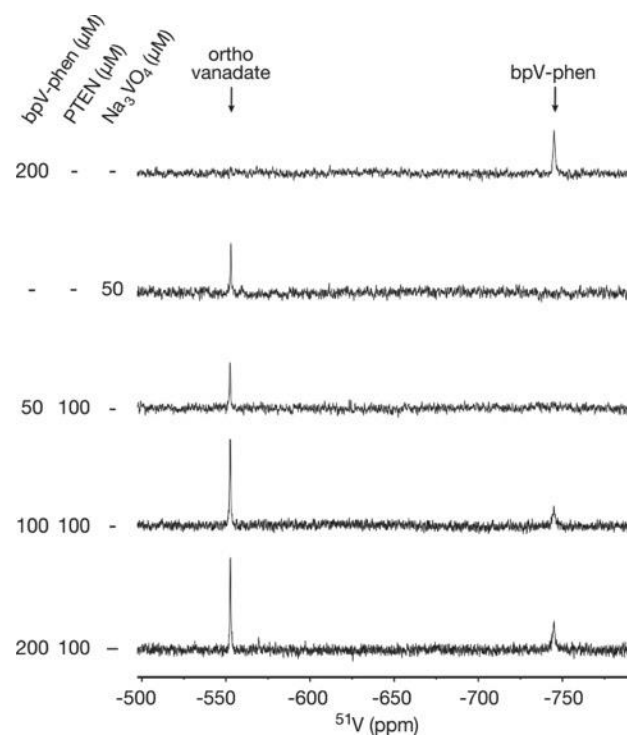


Supporting Figure S17: PTEN undergoes disulfide formation upon treatment with bpV-phen. a) – d) $2F_o - F_c$ electron density omit map in bpV-phen-treated PTEN shows in all four chains a connected electron density between C71 and C124, indicating disulfide formation.

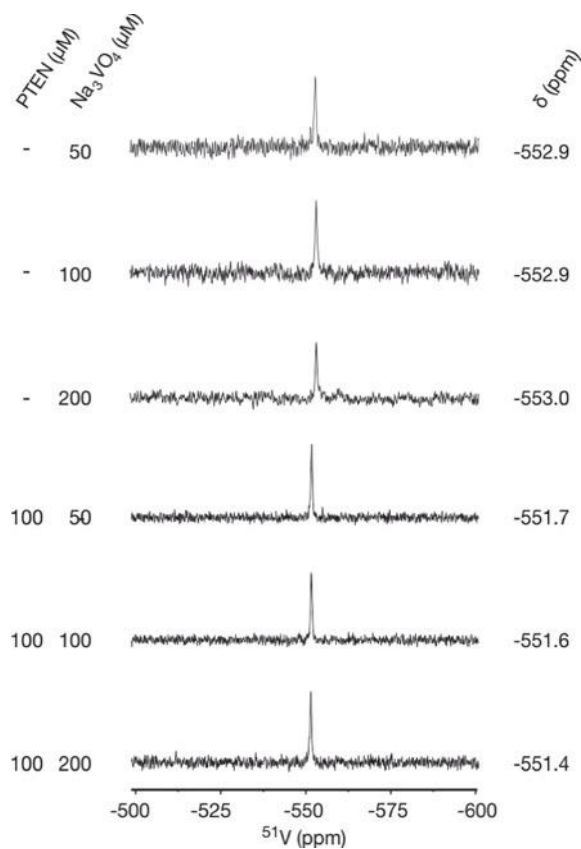


Supporting Figure S18: Comparison of bpV-phen-treated PTEN and reduced PTEN at the active site. a), b) $2 F_o - F_c$ electron density map of the active site in bpV-phen-treated PTEN (orange, a: chain A, b: chain: B). The connected electron density between C71 and C124 indicates disulfide bond formation upon bpV-phen treatment. c) $2 F_o - F_c$ electron density map of the active site in reduced PTEN (gray). The electron density between C71 and C124 is separated and the position of bound tartrate differs from that in oxidized PTEN.

2.5 ^{51}V -NMR measurements



Supporting Figure S19: bpV-phen is converted to orthovanadate. ^{51}V -NMR titration measurements of bpV-phen (50–200 μM) in presence of full-length PTEN (100 μM).



Supporting Figure S20: Orthovanadate shows very low affinity for pre-oxidized PTEN. ⁵¹V-NMR titration measurements of Na₃VO₄ (50–200 μM) in the presence and absence of pre-oxidized full-length PTEN (100 μM). Low affinity of the ligand ($K_D > 1$ mM) is indicated by the absence of line broadening and chemical shift change. High affinity interactions with proteins result in extensive ⁵¹V-NMR peak broadening and chemical shift changes due to changes in correlation time and chemical environment.^[22]

3 REFERENCES

- [1] G. E. Smith, M. D. Summers, M. J. Fraser, *Mol. Cell. Biol.* **1983**, 3, 2156–2165.
- [2] UniProt Consortium, *Nucleic Acids Res.* **2015**, 43, D204–12.
- [3] S. G. Carter, D. W. Karl, *J. Biochem. Biophys. Methods* **1982**, 7, 7–13.
- [4] J. Rappsilber, M. Mann, Y. Ishihama, *Nat. Protoc.* **2007**, 2, 1896–1906.
- [5] A. Michalski, E. Damoc, J.-P. Hauschild, O. Lange, A. Wieghaus, A. Makarov, N. Nagaraj, J. Cox, M. Mann, S. Horning, *Mol. Cell Proteomics* **2011**, 10, M111.011015.
- [6] J. V. Olsen, B. Macek, O. Lange, A. Makarov, S. Horning, M. Mann, *Nat. Methods* **2007**, 4, 709–712.
- [7] J. Cox, M. Mann, *Nat. Biotechnol.* **2008**, 26, 1367–1372.
- [8] W. Kabsch, *Acta Crystallogr. D Biol. Crystallogr.* **2010**, 66, 125–132.
- [9] F. C. Bernstein, T. F. Koetzle, G. J. Williams, E. F. Meyer, M. D. Brice, J. R. Rodgers, O. Kennard, T. Shimanouchi, M. Tasumi, *Ann. Rev. Biochem.* **1977**, 112, 535–542.
- [10] E. Potterton, P. Briggs, M. Turkenburg, E. Dodson, *Acta Crystallogr. D Biol. Crystallogr.* **2003**, 59, 1131–1137.
- [11] M. D. Winn, C. C. Ballard, K. D. Cowtan, E. J. Dodson, P. Emsley, P. R. Evans, R. M. Keegan, E. B. Krissinel, A. G. W. Leslie, A. McCoy, et al., *Acta Crystallogr. D Biol. Crystallogr.* **2011**, 67, 235–242.
- [12] P. Emsley, B. Lohkamp, W. G. Scott, K. Cowtan, *Acta Crystallogr. D Biol. Crystallogr.* **2010**, 66, 486–501.
- [13] G. N. Murshudov, A. A. Vagin, E. J. Dodson, *Acta Crystallogr. D Biol. Crystallogr.* **1997**, 53, 240–255.
- [14] The PyMOL Molecular Graphics System, Version 1.7.4 Schrödinger, LLC.
- [15] P. A. Karplus, K. Diederichs, *Science* **2012**, 336, 1030–1033.
- [16] J. O. Lee, H. Yang, M. M. Georgescu, A. Di Cristofano, T. Maehama, Y. Shi, J. E. Dixon, P. Pandolfi, N. P. Pavletich, *Cell* **1999**, 99, 323–334.
- [17] A. J. Barr, E. Ugochukwu, W. H. Lee, O. N. F. King, P. Filippakopoulos, I. Alfano, P. Savitsky, N. A. Burgess-Brown, S. Müller, S. Knapp, *Cell* **2009**, 136, 352–363.
- [18] S. J. Tsai, U. Sen, L. Zhao, W. B. Greenleaf, J. Dasgupta, E. Fiorillo, V. Orrú, N. Bottini, X. S. Chen, *Biochemistry* **2009**, 48, 4838–4845.
- [19] G. Buhrman, B. Parker, J. Sohn, J. Rudolph, C. Mattos, *Biochemistry* **2005**, 44, 5307–5316.
- [20] D. Barford, A. J. Flint, N. K. Tonks, *Science* **1994**, 263, 1397–1404.
- [21] A. Salmeen, J. N. Andersen, M. P. Myers, T.-C. Meng, J. A. Hinks, N. K. Tonks, D. Barford, *Nature* **2003**, 423, 769–773.
- [22] D. Rehder, M. Časný, R. Grosse, *Magn. Reson. Chem.* **2004**, 42, 745–749.